Journal of Alloys and Compounds 498 (2010) 172–178

Contents lists available at ScienceDirect

Journal of Alloys and Compounds

journal homepage: www.elsevier.com/locate/jallcom

Preparation and *in vitro* evaluation of nanostructured TiO_2/TCP composite coating by plasma electrolytic oxidation

Hongjie Hu[a,b], Xuanyong Liu[a,*], Chuanxian Ding[a]

[a] Key Laboratory of Inorganic Coating Materials, Shanghai Institute of Ceramics, Chinese Academy of Sciences, 1295 Dingxi Road, Shanghai 200050, China
[b] Graduate School of Chinese Academy of Sciences, Beijing 100049, China

ARTICLE INFO

Article history:
Received 11 October 2009
Received in revised form 16 March 2010
Accepted 17 March 2010
Available online 23 March 2010

Keywords:
TiO_2/TCP
Coating
Nanostructured
Bioactivity
Plasma electrolytic oxidation

ABSTRACT

Porous and nanostructured TiO_2/tricalcium phosphate (TCP) composite coating on titanium substrate was prepared by plasma electrolytic oxidation (PEO). The microstructure and phase composition of the coating were characterized using scanning electron microscopy and X-ray diffraction. Its bioactivity was evaluated by simulated body fluid (SBF) immersion tests. MG63 cells were cultured on the surface of the coating to investigate its cytocompatibility. Potentiodynamic polarization tests were applied to measure its corrosion resistance. The results revealed that rough and hydrophilic TiO_2/TCP composite coating with pores of several micrometers and grains of 50–200 nm was prepared by one-step PEO treatment. The TiO_2/TCP composite coating showed good apatite-forming ability in SBF, and the TCP phase in the coating played an important role in inducing apatite formation. MG63 cells could adhere and proliferate on the surface of the coating, indicating its good cytocompatibility. The composite coating also exhibited good corrosion resistance in 0.9% NaCl solution.

1. Introduction

Titanium dioxide (TiO_2) has been widely investigated as bioceramics due to its excellent biocompatibility and corrosion resistance [1]. However, TiO_2 is bio-inert and cannot directly bond to bone immediately after implantation, which limits its applications [2]. Moreover, TiO_2 can generate reactive oxygen species which could pose a serious problem to viability of cells [3–5]. Compositing with bioactive materials is an effective way to overcome these drawbacks [6,7]. Tricalcium phosphate (TCP) has similar inorganic constituents with hard skeletal tissues and shows superior bioactivity and osteoinduction [8,9]. The TiO_2/TCP composite coatings once were prepared using electron beam evaporation [10], sputter deposition [11] and aerosol-deposition [12], respectively. However, most of these methods are hybrid, and the formed coatings exhibit relatively low bond strength. Moreover, they are hardly to produce porous and nanostructured surface which are beneficial to bone tissue in-growth and osteoblast cells adhesion and proliferation [13–16].

Plasma electrolytic oxidation (PEO), so called micro-arc oxidation (MAO), is a relatively convenient technique to deposit ceramic coatings on titanium substrate, and PEO has drawn widely attentions due to the porous, nanostructured and firmly adhered coating characteristics [17–20]. It is an effective and simple way to prepare various functional composite coatings using PEO technology by tailoring the electrolyte compositions and controlling process parameters, and several kinds of composite coatings (such as TiO_2/HA, TiO_2/Al_2O_3 and MgO/ZrO_2) have been prepared in recent few years [21–23]. The PEO coatings reported in literatures usually showed poor apatite-forming ability in simulated body fluid (SBF), and post treatments had to be applied to active the coatings [2,24]. In past, it was rarely explored to prepare the bioactive TiO_2/TCP composite coating by one-step PEO. In this work, bioactive TiO_2/TCP composite coating with porous and nanostructured surface was prepared in a Ca and P-containing electrolyte by PEO treatment. The microstructure and phase composition of the coating were characterized, its bioactivity, cytocompatibility and corrosion resistance were also investigated.

2. Experimental

2.1. Sample preparation

Commercially available pure titanium (purity > 99.85%, Grade 1, Baoji Shi Shenghua Non-ferrous Metal Materials Co., Ltd, China) plates of 10 mm × 10 mm × 2 mm in size were used as substrates, which were ground with 400 # and 1000 # abrasive paper and then ultrasonically washed with acetone, ethyl alcohol and distilled water in an ultrasonic bath prior to PEO treatment. The specimens were fabricated by PEO equipment (MAO30, Pulsetech, China) in two kinds of electrolytes, respectively. One contained 0.05 mol/L glycerophosphate disodium salt pentahydrate ($GPNa_2$, $C_3H_7Na_2O_6P{\cdot}5H_2O$, chemical pure reagent, Kelong Chemical Reagent Plant in Chengdu, China) and 0.1 mol/L calcium acetate monohydrate (CA, $C_4H_6O_4Ca{\cdot}H_2O$, analytical reagent, Sinopharm Chemical Reagent Co.,

* Corresponding author. Tel.: +86 21 52412409; fax: +86 21 52412409.
E-mail address: xyliu@mail.sic.ac.cn (X. Liu).

0925-8388/$ – see front matter © 2010 Elsevier B.V. All rights reserved.
doi:10.1016/j.jallcom.2010.03.147

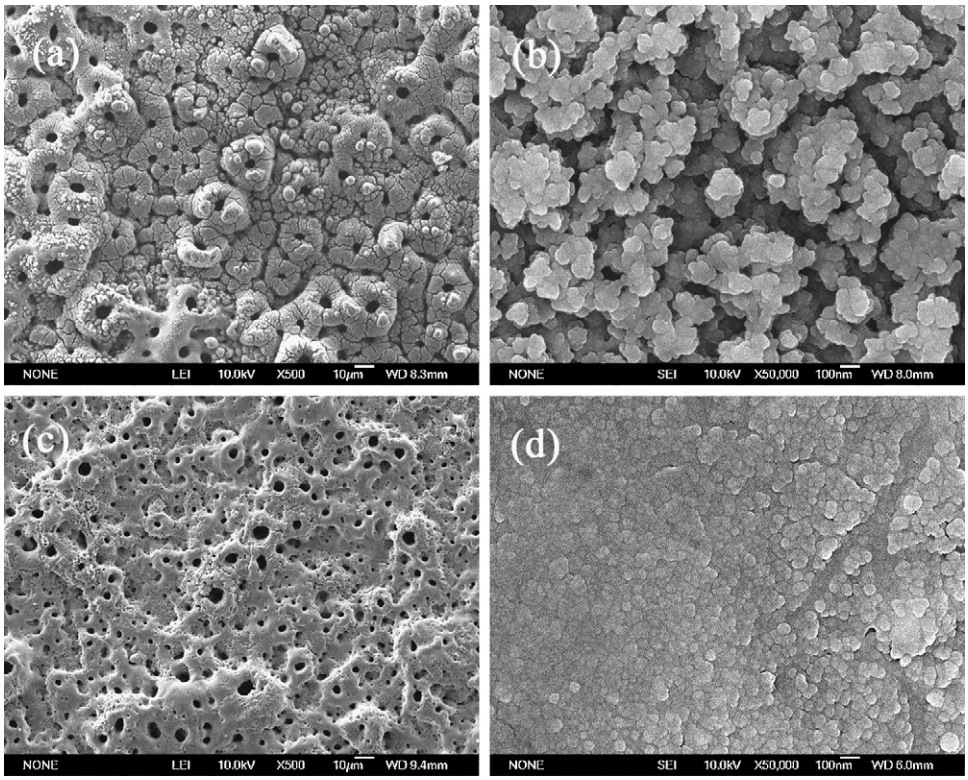

Fig. 1. Surface morphologies of the PEO (a and b) and C-PEO (c and d) coatings in different magnifications.

Ltd, Shanghai, China), and the other contained the same components and 0.1 mol/L ethylene-diamine tetraacetic acid disodium salt (EDTA-2Na, $C_{10}H_{14}N_2Na_2O_8{\cdot}2H_2O$, analytical reagent, Sinopharm Chemical Reagent Co., Ltd, Shanghai, China). The applied current density, frequency, duty cycle and duration time were 33 A/dm^2, 800 Hz, ±10% and 4 min, respectively. Ti plate was used as an anode, and a spiral steel pipe was used as a cathode while it was also used as a dwelling water pipe to sustain the temperature of the electrolyte less than 30 °C in the electrolytic cell. A magnetic stirrer was used to keep the uniform of the components and temperature of the electrolytes. After PEO treatment, the samples were washed with deionized water and dried in air. The samples prepared in the electrolyte without EDTA-2Na were labeled as "PEO coating" while the other samples prepared in EDTA-2Na-containing electrolyte were labeled as "C-PEO coating".

The granules in the electrolyte without EDTA-2Na were collected and heat-treated in a furnace at 400 °C for 4 h. The PEO coating was soaked in 300 mL deionized water for 8 days and ultrasonically cleaned for 20 min every other day. The water was refreshed every 2 days, too. The ultrasonically cleaned PEO coating was labeled as "US-PEO coating".

2.2. Bioactivity evaluation

The samples were immersed in simulated body fluid (SBF) for 14 and 28 days to evaluate their bioactivity. The SBF was prepared by dissolving reagent-grade chemicals of NaCl, $NaHCO_3$, KCl, $K_2HPO_4{\cdot}3H_2O$, $MgCl_2{\cdot}6H_2O$, $CaCl_2$, and Na_2SO_4 in deionized water and buffered at pH 7.4 with tris-hydroxymethyl-aminomethane (Tris) and HCl at 36.5 °C [25]. A couple of samples immersed in a plastic vial containing 50 mL of SBF were kept under static conditions inside a biological thermostat at 36.5 °C. The SBF was refreshed every other week so that the lack of ions would not inhibit the apatite formation. After immersed for designed days, the samples were removed from the SBF, gently washed with deionized water and dried at 40 °C. The immersion tests were conducted in triplicate using different samples to ensure the validity of the results.

2.3. Cell culture

Osteoblast-like cell line MG63 (Cells Resource Center of Shanghai Institutes for Biological Science, China) was used to evaluate the cytocompatibility of the PEO and C-PEO coatings. Samples sterilized by γ-irradiation were put into 24-well culture plates (Costar, USA). Then l.0 mL cell suspension with cell density of 1×10^5 cell/mL was added into each well. Culture plate was transformed gently to an incubator of 37 °C. After cultured for 1, 3 and 7 days, the samples were taken out, rinsed with a phosphate buffered saline solution (pH 7.2, PBS) twice to remove unattached cells, and than fixed with 2.5% glutaraldehyde solution in a sodium cacodylate buffer (pH 7.4, Gibco, Invitrogen) for 30 min. The samples were then dehydrated in a grade ethanol series (30, 50, 75, 90, 95 and 100%, v/v) for 10 min, respectively, with final dehydration conducted in absolute ethanol twice followed by drying in the hexamethyldisilizane ethanol solution series. After gold sputtering, the cell morphology was observed by scanning electron microscopy (SEM) [26].

2.4. Corrosion resistance evaluation

The corrosion resistance of the PEO and C-PEO coatings as well as commercially pure titanium plates (CP-Ti) were evaluated by potentiodynamic polarization tests through CHI760C electrochemical analyzer (Chenhua, China) in physiological saline (0.9% NaCl solution). The measurement was conducted using a conventional three electrodes electrochemical cell with a saturated calomel electrode as the reference electrode, a graphite rod as the counter electrode, and the sample with the area of 0.3 cm^2 as the working electrode. All electrochemical tests were conducted at room temperature with a scanning rate of 20 mV/min. Four samples of each group were tested, respectively, and the average values of four measured data were presented.

2.5. Characterization

The phase composition of the samples was analyzed by X-ray diffraction (XRD, D/MAX-2550, Rigaku, Japan) at 40 kV and 100 mA. Their surface morphologies were determined by field-emission scanning electron microscopy (FE-SEM, JSM-6700F, JEOL, Japan). The elemental composition of the samples was measured by energy-dispersive X-ray spectrometry (EDS) attached to electron probe X-ray microanalysis system (EPMA, JAX-8100, Japan). The surface roughness of the samples was quantified using a surface profiler (HOMMEL TESTER T8000, Wave, Germany) with a scan distance of 4.8 mm and scan rate of 0.5 mm/s. Contact angles were measured using a contact angle instrument (SL200B, Solon, China). A few micrograms of the newly formed layer on PEO coating immersed in SBF for 28 days were scraped off, mixed with KBr and pressed for structural analysis by Fourier transfer infrared spectroscopy (FT-IR, Nicolet Nexus, USA). The PEO and C-PEO coatings were immersed in Tris–HCl buffer solution (buffered at pH 7.4 with Tris and HCl at 36.5 °C) for 1, 3, 5, 7 and 9 days, respectively, and the Ca and P concentrations of the buffer solution were measured by an inductively coupled plasma/optical emission spectroscopy (ICP-OES, Vista AX, Varian, USA). The EDS, surface roughness and contact angle tests were conducted three times at different places on each sample to ensure the validity of the data.

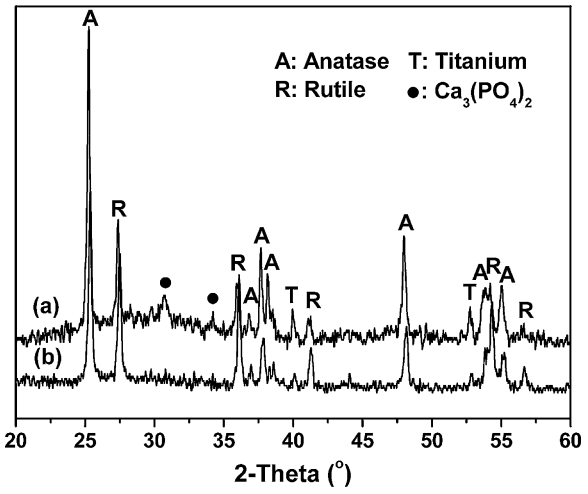

Fig. 2. XRD patterns of the PEO (a) and C-PEO (b) coatings.

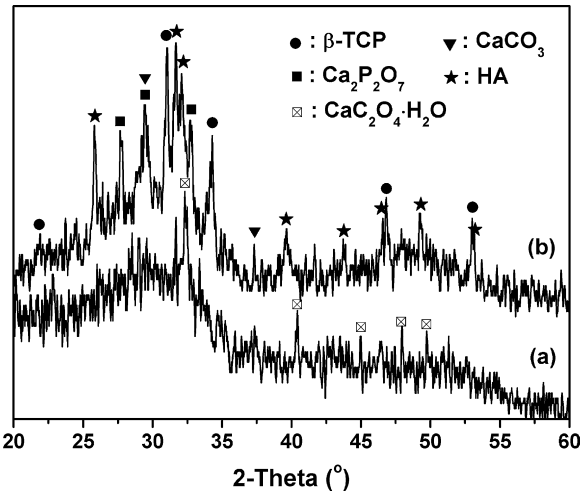

Fig. 3. XRD patterns of the as-collected granules in the electrolyte without EDTA-2Na (a) and those heat-treated at 400 °C for 4 h (b).

3. Results and discussion

3.1. Microstructure and phase composition of coatings

Fig. 1 shows the surface morphologies of the PEO and C-PEO coatings. It is clear that both coatings are porous with pore size of several micrometers. These pores are well separated and homogeneously distributed over the coatings. High magnification views show that the grains on PEO coating surface are about 50–200 nm, while the grains on C-PEO coating surface are about 20–100 nm in diameter. The surface roughness (Ra) of the PEO and C-PEO coatings are 3.3 ± 0.2 and 2.0 ± 0.2 μm, respectively. The water contact angle value of the PEO coating is nearly 0°, while it is 25.03 ± 3.32° for C-PEO coating, implying that both PEO and C-PEO coatings are rough and hydrophilic. The higher surface roughness and lower contact angle of the PEO coating may be ascribed to the looser coating surface, as shown in Fig. 1.

The elemental composition of the PEO and C-PEO coatings detected by EDS are summarized in Table 1. Both coatings mainly contain Ti, Ca, P and O elements. More Ca and P, but less Ti is detected in PEO coating than in C-PEO coating, indicating that PEO coating is Ca–P rich. The XRD patterns of the PEO and C-PEO coatings are shown in Fig. 2. Both PEO and C-PEO coatings mainly contain anatase (JCPDS # 21-1272) and rutile (JCPDS # 21-1276) phases. The feature peaks of $Ca_3(PO_4)_2$ (TCP, JCPDS # 09-0169) are observed in the XRD pattern of PEO coating (Fig. 2a), while it is not found in the XRD pattern of C-PEO coating (Fig. 2b).

For explaining the phase composition difference of the PEO and C-PEO coatings, the characteristics of the two electrolytes were supposed to be referred. There were some milky granules in the electrolyte without EDTA-2Na. The XRD patterns of the granules are shown in Fig. 3. The as-collected powders are mainly amorphous and only contain a little amount of $CaC_2O_4{\cdot}H_2O$. After heat-treated at 400 °C for 4 h, feature peaks of TCP, HA, $CaCO_3$ and $Ca_2P_2O_7$ are detected, suggesting that the granules mainly are Ca–P compound. The formation of the granules may be ascribed to the hydrolysis of $GPNa_2$ [27] and dissolution of CO_2 in air:

$$Ca(CH_3COO)_2 \rightarrow Ca^{2+} + 2(CH_3COO)^- \quad (1)$$

$$Na_2C_3H_5(OH)_2PO_4 + H_2O \rightarrow C_3H_5(OH)_3 + PO_4^{3-} + H^+ + 2Na^{2+} \quad (2)$$

$$CO_2 + H_2O \rightarrow CO_3^{2-} + 2H^+ \quad (3)$$

$$3Ca^{2+} + 2PO_4^{2-} \rightarrow Ca_3(PO_4)_2\downarrow \quad (4)$$

$$Ca^{2+} + CO_3^{2-} \rightarrow CaCO_3\downarrow \quad (5)$$

It was inferred that the stirring and electro-migration during the PEO process brought the granules in electrolyte onto the surface of the anode, where dielectric breakdown process occurred incessantly, and deposited on the coating surface. This process is similar to PEO coupled with electrophoretic deposition process [28]. The plasma arc produced locally high temperature surrounding the anode sintered the coating, accelerated its crystallization and resulted in the formation of the TiO_2/TCP composite coating.

On the other hand, no precipitate was observed in the electrolyte with EDTA-2Na, which may be ascribed to the chelation of EDTA-2Na [29]:

$$Ca^{2+} + H_2Y^{2-} \rightarrow [CaY^{2-}] + 2H^+ \quad (Y = [_2(OOC)NCH_2CH_2N(COO)_2]^{4-}) \quad (6)$$

The Ca^{2+} ions were depleted by the chelation reaction because the concentrations of CA and EDTA-2Na in the electrolyte both were 0.1 mol/L, which prevented the production of TCP and $CaCO_3$. The negatively charged CaY^{2-} and PO_4^{3-} ions in the electrolyte moved to the anode under the applied electrical field and the Ca and P elements were incorporated into the C-PEO coating. The different formation mechanisms resulted in the different phase compositions of the PEO and C-PEO coatings.

Table 1
Elemental composition of the PEO, C-PEO and US-PEO coatings detected by EDS.

Sample	Elemental composition (wt.%)			
	Ca	P	Ti	O
PEO coating	21.64 ± 0.39	15.08 ± 0.38	21.08 ± 0.41	42.20 ± 0.50
C-PEO coating	13.63 ± 0.30	12.47 ± 0.31	31.71 ± 0.45	42.18 ± 0.47
US-PEO coating	9.48 ± 0.33	5.79 ± 0.27	49.11 ± 1.12	35.63 ± 1.41

3.2. Bioactivity and solubility of coatings

The surface morphologies of the PEO coating immersed in SBF for 14 and 28 days are shown in Fig. 4a and b, respectively. It is clear that the surface of the PEO coating was partially covered by a newly formed layer after incubated in SBF for 14 days (Fig. 4a). Higher magnification image shows that the newly formed layer with worm-like grains of ~100 nm in diameter is observed. After immersed in SBF for 28 days, the coating was fully covered by a dense precipitate layer. The higher magnification image shows that the layer is a network structure which consisted of numerous flakes of ~20 nm in thickness (Fig. 4b). The XRD pattern of the PEO coating

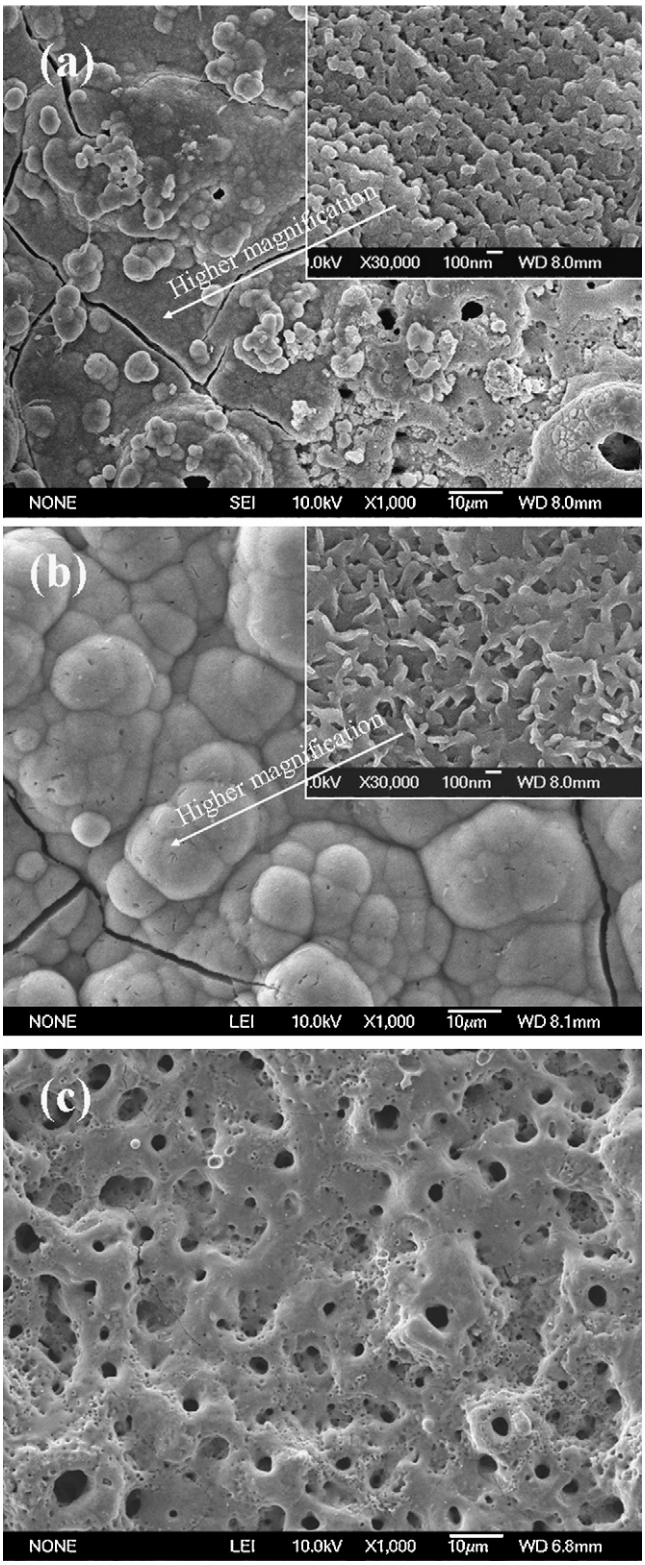

Fig. 4. SEM micrographs of the PEO coating after immersed in SBF for 14 (a) and 28 (b) days; (c) SEM morphology of the C-PEO coating after immersed in SBF for 28 days.

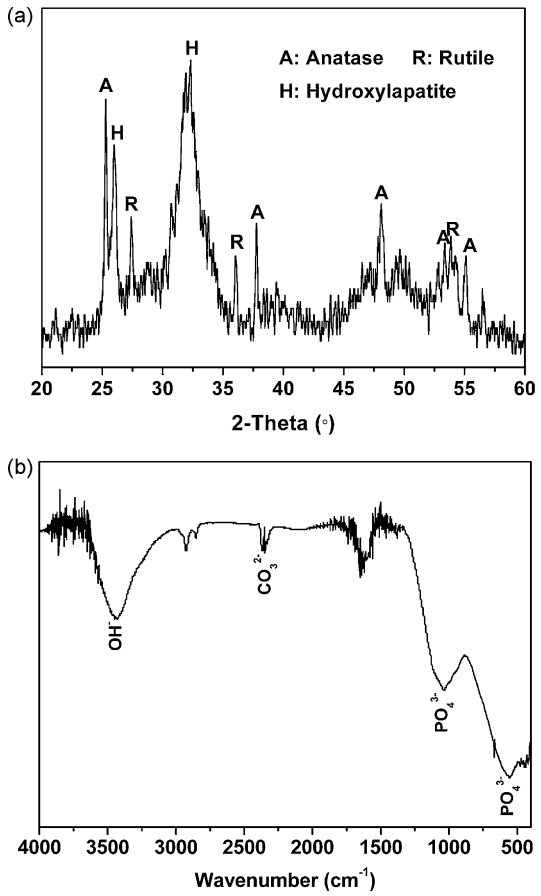

Fig. 5. XRD pattern (a) and FT-IR spectrum (b) of the newly formed layer on PEO coating after immersed in SBF for 28 days.

soaked in SBF for 28 days are shown in Fig. 5a. The feature peaks of HA are clearly detected. FT-IR spectrum (Fig. 5b) shows the feature absorption bands of PO_4^{3-}, OH^- and CO_3^{2-}. EDS analysis reveals that the Ca/P ratio of the newly formed layer is 1.41 ± 0.23, indicating that the newly formed layer is Ca-deficient carbonated HA (bone-like apatite). The surface morphology of the C-PEO coating immersed in SBF for 28 days is shown in Fig. 4c. It still appears porous without any precipitate, suggesting the poor bioactivity of the C-PEO coating.

It is well known that TCP usually shows high bioactivity and solubility [8,9,30]. The TCP phase in PEO coating may significantly contribute to its bioactivity and solubility. For comparison, the PEO coating was ultrasonically cleaned to remove the TCP phase and the US-PEO coating was obtained. The XRD pattern and surface morphologies of US-PEO coating before and after immersed in SBF are shown in Fig. 6. The US-PEO coating also consists of anatase and rutile phases, but no TCP phase is detected, indicating that the TCP phase is removed from the coating by ultrasonically cleaning. The Ca and P contents of the US-PEO coating are also evidently lower than the PEO coating (Table 1). No precipitation formed on the surface of the US-PEO coating soaked in SBF for 28 days, suggesting its poor bioactivity. The results reveal that the TCP phase in PEO coating plays an important role in inducing apatite formation in SBF.

The Ca and P concentrations of the Tris-HCl buffer solution after immersion of the PEO, C-PEO and US-PEO coatings for different periods are shown in Fig. 7. It is suggested that once the samples are immersed in the solution, Ca and P begin to release from the coating, and the concentrations became higher and higher with duration of the immersion time. The Ca and P concentrations of the buffer solution after immersion of the PEO coating are significantly higher than the other two solutions after immersion of the C-PEO and US-PEO coatings, which is thought to be related to the TCP phase in PEO coating due to its high solubility [30]. The higher solubility of the PEO coating results in higher Ca, P concentration at

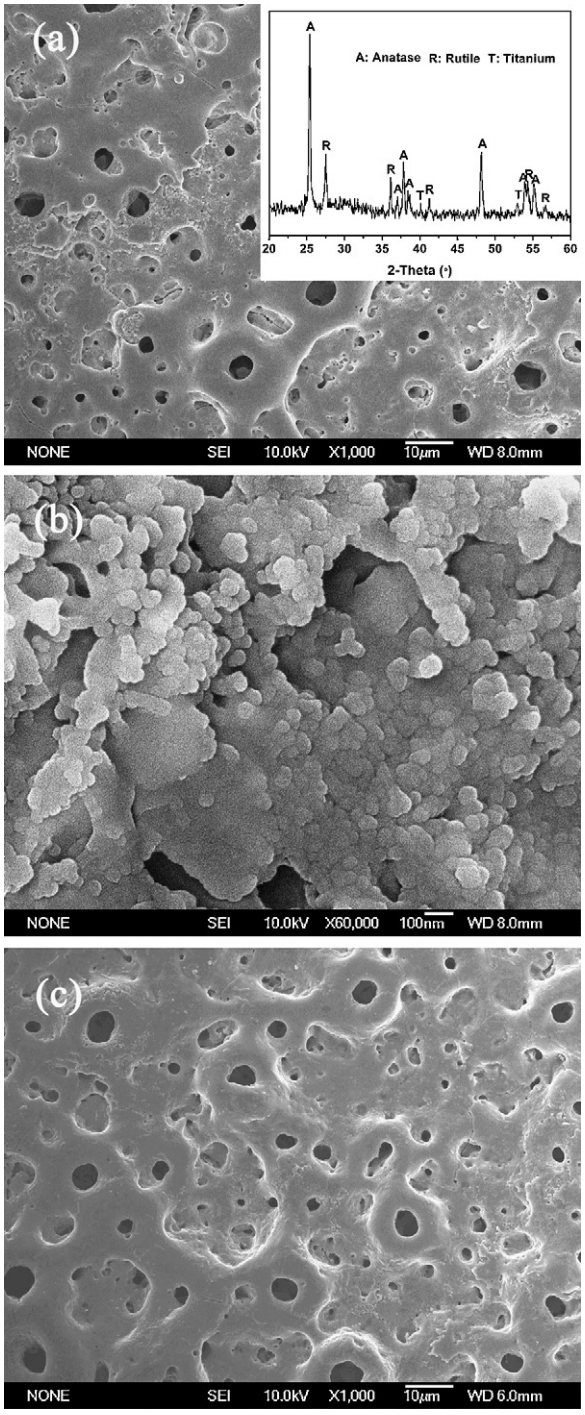

Fig. 6. Surface morphologies of the (a) US-PEO coating (insert indicating its XRD pattern); (b) higher magnification of (a); (c) after immersed in SBF for 28 days.

the early stage of the incubation in SBF, which would increase the degree of super saturation of SBF. Once the Ca and P concentrations reach the critical nucleation concentration of apatite, it triggers the apatite nucleation and grow spontaneously by assembling the remaining calcium, phosphate and hydrogen carbonate ions around apatite nuclei in SBF [31]. The SBF with immersion of the C-PEO and US-PEO coatings are hard to reach the critical nucleation concentration of apatite because of their low Ca, P content and solubility, and result in the poor bioactivity of the C-PEO and US-PEO coatings.

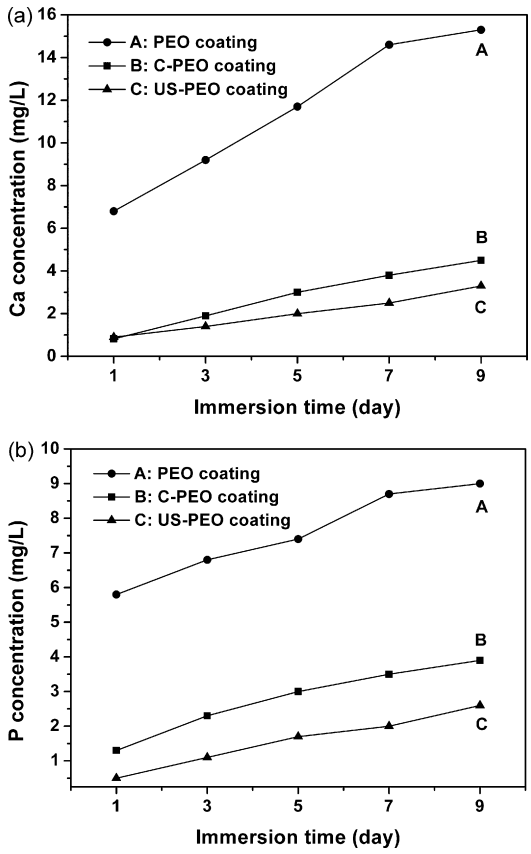

Fig. 7. Ca (a) and P (b) concentrations of the Tris–HCl buffer solution with immersion of the PEO, C-PEO and US-PEO coatings for various days.

3.3. Cytocompatibility

The morphologies of MG63 cells cultured on PEO and C-PEO coatings for 1, 3 and 7 days are shown in Fig. 8. After 1 day of culture, the MG63 cells on PEO and C-PEO coatings exhibited good adhesion and spread out uniformly over the coatings, and displayed numerous filopodia extensions. After 3 days of culture, the cells spread to the whole surface and grew layer by layer. Extending the culture time to 7 days, all MG63 cells spread with numerous filopodia and fused to form a complete layer on the coatings, indicating that both PEO and C-PEO coatings are favorable for the adhesion and proliferation of MG63 cells and show good cytocompatibility.

It is generally accepted that high surface roughness of a material leads to enhanced cell adhesion and proliferation [32]. A low contact angle also leads to high surface energy, which is another factor that contributes to better cell attachment [33]. It also has been reported that a porous structure of an implant is beneficial to bone tissue in-growth and osteoblast cells invasion, adhesion and proliferation [13,14]. Nanophase ceramics have also been reported can enhance proteins interaction (such as adsorption, configuration, bioactivity, etc.) and subsequent osteoblast adhesion [15,16]. Both PEO and C-PEO coatings are not only rough and hydrophilic but also porous and nanostructured, which are thought to be the reasons for their good cytocompatibility and no cytotoxicity.

3.4. Corrosion resistance

Once biomaterials are implanted into the body, electrochemical corrosion inevitably occurs in the physiological environment and greatly influences the biocompatibility and service life of the implants. In order to evaluate the corrosion resistance of the PEO and C-PEO coatings, corrosion immersion tests were carried out.

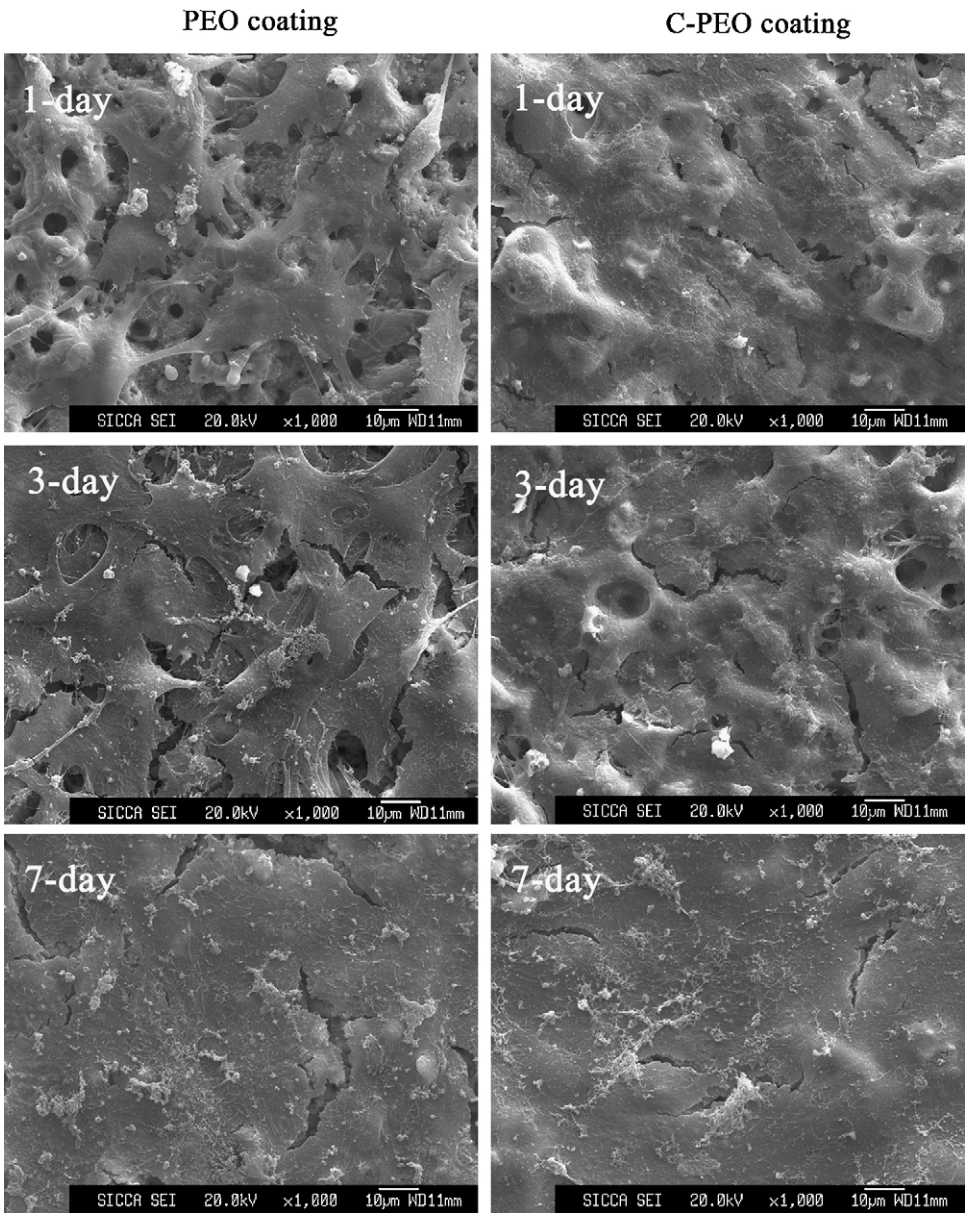

Fig. 8. Morphologies of MG63 cells cultured on the PEO and C-PEO coatings for 1, 3 and 7 days, respectively.

The potentiodynamic polarization curves of the PEO and C-PEO coatings in 0.9% NaCl solution are shown in Fig. 9. For comparison, CP–Ti plates were also applied. The potentiodynamic polarization curves of the PEO and C-PEO coatings are rather near, indicating that their corrosion resistance are comparable, and the small amount of TCP in PEO coating does not depress its corrosion resistance. Comparing with CP-Ti, the corrosion resistance of the PEO and C-PEO coatings both are apparently higher, which can be observed by a shift of polarization curves toward the region of higher potential. The corrosion potential values of the PEO and C-PEO coatings are about -0.262 ± 0.034 and -0.267 ± 0.026 V, respectively, which are higher than -0.302 ± 0.051 V for CP-Ti. The good corrosion resistance of the PEO and C-PEO coatings may be ascribed to the TiO_2-based ceramic coatings on titanium which usually show superior corrosion resistance [34]. The good corrosion resistance of the PEO coatings may improve the long term stability and service life of the implants in biological environment.

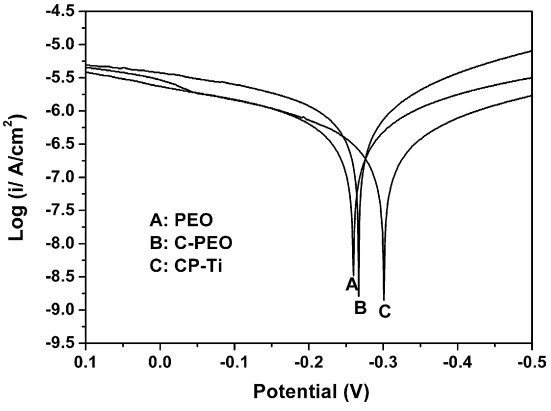

Fig. 9. Potentiodynamic polarization curves of the PEO and C-PEO coatings as well as CP-Ti in 0.9% NaCl solution.

4. Conclusions

TiO_2-based ceramic coatings with porous and nanostructured surfaces were prepared by plasma electrolyte oxidation in electrolytes without and with EDTA-2Na (PEO and C-PEO), respectively. The PEO coating mainly contained anatase, rutile and TCP phases with grains of about 50–200 nm in diameter, while no TCP phase was detected in the C-PEO coating. The PEO coating could introduce apatite to precipitate on its surface in SBF, indicating its good bioactivity, while the C-PEO coating was bio-inert. The TCP phase in PEO coating played an important role in inducing apatite formation. MG63 cells could adhere and proliferate on the surface of the PEO and C-PEO coatings, indicating their good cytocompatibility. Both PEO and C-PEO coatings exhibited good corrosion resistance in 0.9% NaCl solution. Such porous and nanostructured TiO_2/TCP composite coating is expected to be used as orthopedic and implant materials.

Acknowledgements

This work was jointly supported by Shanghai Science and Technology R&D Fund under grant 0952nm04400, 07JC14057, 0852nm03300 and 08ZR1421600, National Basic Research Fund under grant 2005CB623901, National Natural Science Foundation of China 30700170, Shanghai-Unilever Research and Development Fund 09520715200.

References

[1] X.Y. Liu, X.B. Zhao, B.E. Li, C. Cao, Y.Q. Dong, C.X. Ding, et al., Acta Biomater. 4 (2008) 544–552.
[2] Y. Han, D.H. Chen, J.F. Sun, Y.M. Zhang, Acta Biomater. 4 (2008) 1518–1529.
[3] L.F. Liu, J. Barford, K.L. Yeung, J. Environ. Sci. Chin. 21 (2009) 700–706.
[4] K.L. Yeung, W.K. Leung, N. Yao, S.L. Cao, Catal. Today 143 (2009) 218–224.
[5] S.L. Cao, K.L. Yeung, J.K.C. Kwan, P.M.T. To, S.C.T. Yu, Appl. Catal. B 86 (2009) 127–136.
[6] X.F. Xiao, R.F. Liu, Y.Z. Zheng, Surf. Coat. Technol. 200 (2006) 4406–4413.
[7] X.Y. Liu, C.X. Ding, Biomaterials 23 (2002) 4065–4077.
[8] R.Z. LeGeros, Chem. Rev. 108 (2008) 4742–4753.
[9] S.V. Dorozhkin, M. Epple, Angew. Chem. Int. Ed. 41 (2002) 3130–3146.
[10] Y. Li, I.S. Lee, F.Z. Cui, S.H. Choi, Biomaterials 29 (2008) 2025–2032.
[11] A.R. Boyd, H. Duffy, R. McCann, B.J. Meenan, Mater. Sci. Eng. C 28 (2008) 228–236.
[12] J. Ryu, K.-Y. Kim, B.-D. Hahn, J.-J. Choi, W.-H. Yoon, B.-K. Lee, et al., Catal. Commun. 10 (2009) 596–599.
[13] K. Das, S. Bose, A. Bandyopadhyay, Acta Biomater. 3 (2007) 573–585.
[14] F.A. Akin, H. Zreiqat, S. Jordan, M.B. Wijesundara, L. Hanley, J. Biomed. Mater. Res. 57 (2001) 1803–1810.
[15] G. Balasundaram, T.J. Webster, J. Mater. Chem. 16 (2006) 3737–3745.
[16] T.J. Webster, C. Ergun, R.H. Doremus, R.W. Siegel, R. Bizios, Biomaterials 21 (2000) 1803–1810.
[17] L. Wang, L. Chen, Z.C. Yan, H.L. Wang, J.Z. Peng, J. Alloys Compd. 493 (2010) 445–452.
[18] J. He, Q.Z. Cai, Y.G. Ji, H.H. Luo, D.J. Li, B. Yu, J. Alloys Compd. 482 (2009) 476–481.
[19] F. Liua, J.L. Xu, D.Z. Yu, F.P. Wang, L.C. Zhao, J. Alloys Compd. 487 (2009) 391–394.
[20] Z.P. Yao, Y.J. Xu, Z.H. Jiang, F.P. Wang, J. Alloys Compd. 488 (2009) 273–278.
[21] M.S. Kim, J.J. Ryu, Y.M. Sung, Electrochem. Commun. 9 (2007) 1886–1891.
[22] J.L. Xu, F. Liu, F.P. Wang, D.Z. Yu, L.C. Zhao, J. Alloys Compd. 472 (2009) 276–280.
[23] H.H. Luo, Q.Z. Cai, B.K. Wei, B. Yu, J. He, D.J. Li, J. Alloys Compd. 474 (2009) 551–556.
[24] W.-H. Song, H.S. Ryu, S.-H. Hong, J. Am. Ceram. Soc. 89 (2005) 2642–2644.
[25] T. Kokubo, H. Takadama, Biomaterials 27 (2006) 2907–2915.
[26] G.C. Wang, X.Y. Liu, J.H. Gao, C.X. Ding, Acta Biomater. 6 (2009) 2270–2278.
[27] A.L. Yerokhin, X. Nie, A. Leyland, Surf. Coat. Technol. 122 (1999) 73–93.
[28] D.Y. Kim, M. Kim, H.E. Kim, Y.H. Koh, H.W. Kim, J.H. Jang, Acta Biomater. 5 (2009) 2196–2205.
[29] V.M. Frauchiger, F. Schlottig, B. Gasser, M. Textor, Biomaterials 25 (2004) 593–606.
[30] X. Wei, O. Ugurlu, A. Ankit, H.Y. Acar, M. Akinc, Mater. Sci. Eng. C 29 (2009) 126–135.
[31] T. Kokubo, H.M. Kim, M. Kawashita, Biomaterials 24 (2003) 2161–2175.
[32] K. Hatano, H. Inoue, T. Kojo, T. Matsunaga, et al., Bone 25 (1999) 439–445.
[33] K. Webb, V. Hlady, P.A. Tresco, J. Biomed. Mater. Res. 41 (1998) 422–430.
[34] P. Shi, W.F. Ng, M.H. Wong, F.T. Cheng, J. Alloys Compd. 469 (2009) 286–292.